

# Multiple intrinsically identical single photon emitters in the solid-state

L. J. Rogers,<sup>1</sup> K. D. Jahnke,<sup>1</sup> T. Teraji,<sup>2</sup> L. Marseglia,<sup>1</sup> C. Müller,<sup>1</sup> B. Naydenov,<sup>1</sup>  
H. Schauffert,<sup>1</sup> C. Kranz,<sup>3</sup> J. Isoya,<sup>4</sup> L. P. McGuinness,<sup>5</sup> and F. Jelezko<sup>5</sup>

<sup>1</sup>*Institute for Quantum Optics and Center for Integrated Quantum  
Science and Technology (IQ<sup>st</sup>), University Ulm, D-89081 Germany*

<sup>2</sup>*National Institute for Materials Science, 1-1 Namiki, Tsukuba, Ibaraki 305-0044, Japan*

<sup>3</sup>*Institute of Analytical and Bioanalytical Chemistry, University Ulm, D-89081 Germany*

<sup>4</sup>*Research Center for Knowledge Communities, University of Tsukuba, 1-2 Kasuga, Tsukuba, Ibaraki 305-8550, Japan*

<sup>5</sup>*Institute for Quantum Optics and Center for Integrated Quantum  
Science and Technology (IQ<sup>st</sup>), University Ulm, D-89081 Germany*

(Dated: September 25, 2018)

Emitters of indistinguishable single photons are crucial for the growing field of quantum technologies [1–3]. To realize scalability and increase the complexity of quantum optics technologies, multiple independent yet identical single photon emitters are also required. However typical solid-state single photon sources are inherently dissimilar, necessitating the use of electrical feedback [4–6] or optical cavities [7] to improve spectral overlap between distinct emitters. Here, we demonstrate bright silicon-vacancy ( $\text{SiV}^-$ ) centres in low-strain bulk diamond which intrinsically show spectral overlap of up to 91% and near transform-limited excitation linewidths. Our results have impact upon the application of single photon sources for quantum optics and cryptography, and the production of next generation fluorophores for bio-imaging.

Single, transform-limited photons are an essential resource for many quantum interference experiments, since indistinguishability between photons allows path-of-origin information to be erased. This makes possible investigation of fundamental quantum optics phenomena which have applications in quantum imaging [8], quantum computing [1] and quantum repeaters [2]. Interactions between indistinguishable photons from multiple emitters can also be used to create entangled quantum states over macroscopic physical distances [3]. However, to date it has proved difficult to achieve indistinguishability between distinct single photon sources.

Individual trapped ions in vacuum are a natural source of identical photons, limited primarily by their independent motion [9], whereas in the solid-state it has been necessary to use optical cavities and/or electrical tuning in order to interfere photons from distinct emitters [10]. In particular, quantum dots and single molecules have demonstrated transform-limited linewidths over short timescales, allowing interference between photons from the same emitter [7, 11] and physically separated emitters [4]. Colour centres in diamond, located deep within an ultrapure lattice, show excellent photostability and are attractive single photon sources. The negative nitrogen vacancy ( $\text{NV}^-$ ) centre is well studied and has been used for early photonics applications [12, 13], but its broad spectral emission is ill-suited to single photon technologies [3].

The negative silicon-vacancy ( $\text{SiV}^-$ ) centre has promising spectral properties [14–16]. It has a strong optical transition with a prominent zero-phonon line (ZPL) at 737 nm and only a weak phonon sideband [17–21]. Structurally, it is comprised of a silicon atom located between adjacent vacancies in the diamond lattice [15, 22, 23] (Figure 1a). The strong ZPL has sparked interest, but large variation in spectral properties between individual

sites [16] has limited the value of  $\text{SiV}^-$  as a single photon emitter.

Here we obtain highly uniform, narrow linewidths by using low strain, high-pressure, high-temperature (HPHT) diamond as a substrate of high crystalline quality. A layer of ultrapure diamond was overgrown on this (001)-oriented substrate with chemical vapour deposition (CVD), allowing precise control of impurity concentrations. Silicon was introduced to the plasma and incorporated into the diamond at concentrations below 1 ppb (see Methods). Single  $\text{SiV}^-$  defects formed during growth were observed by fluorescence confocal microscopy (Figure 1b,c). Photon antibunching measurements provided confirmation of single photon emission.

At 4 K the ZPL consists of four lines as a result of optically allowed transitions between doublet ground and excited states [24, 25] (Figure 2a,b). Each of these transitions was resonantly excited and fluorescence was detected in the sideband. Scanning the laser frequency produced photoluminescence excitation (PLE) spectra, shown for a single emitter in Figure 2c.

The pair of lines at shorter wavelengths (higher energy), here labelled lines A and B, had full-width at half maximum (FWHM) of 352 and 409 MHz. The pair of lines at longer wavelengths were considerably narrower at 136 MHz (line C) and 119 MHz (line D). All of these PLE spectra were recorded at minimal laser intensities to avoid power-broadening. In order to compare these linewidths to their expected transform-limit, pulsed 532 nm excitation was used to measure the excited-state lifetime for several individual  $\text{SiV}^-$  centers (Figure 2c). A decay time of  $1.72 \pm 0.04$  ns was measured at 4 K. Our measured result for line D is therefore only 26% over the transform-limited linewidth of 94 MHz.

It is important to account for the extra width of lines A and B, and further information is provided by photolu-

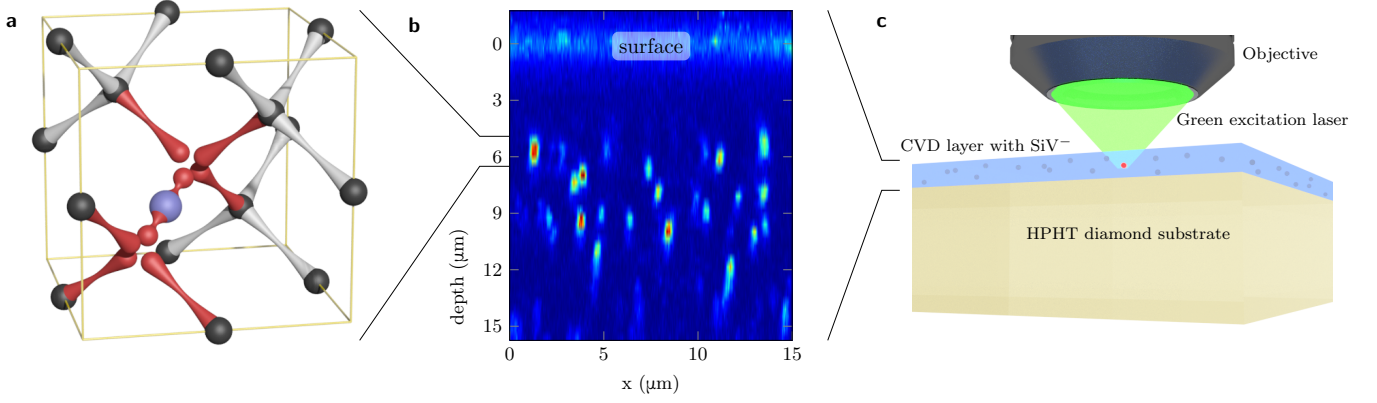


FIG. 1. Silicon vacancy centers in diamond. **a.** Physical structure of the  $\text{SiV}^-$  centre in the diamond lattice, with a silicon atom lying in between adjacent vacancies. **b.** Fluorescence confocal image showing the depth profile of single  $\text{SiV}^-$  centres beneath the diamond surface (corrected for refractive index). **c.** The  $\text{SiV}^-$  centres were present in a single crystal CVD diamond layer, and had been incorporated during growth due to silicon doping of the plasma. The CVD layer was grown homoepitaxially on low strain, high-pressure, high-temperature diamond substrates and investigated from the top.

minescence (PL) measured with a spectrometer. At 4 K lines C and D are much brighter than the higher energy lines (Figure 2a), which correspond to transitions from the upper branch of the excited state (Figure 2b). With increasing temperature these lines gain relative intensity, indicating that thermal relaxation occurs in the  $\text{SiV}^-$  excited state. The downward exchange rate  $\Gamma_\downarrow$  adds to the rate of decay to the ground state and reduces the effective lifetime of the upper branch. Consequently, lines A and B are broadened and lose intensity in PL. The upward exchange rate  $\Gamma_\uparrow = \Gamma_\downarrow \exp \frac{\Delta E}{k_B T}$  depends on the Boltzmann factor, making it small but still measurable at 4 K. This additional rate out of the lower branch accounts for half of the extra linewidth above the transform-limit for lines C and D.

At 4 K, 71% of the total ZPL fluorescence is contained in line C. Combined with the Debye-Waller factor of 70% [26], this means that half of the total  $\text{SiV}^-$  fluorescence is emitted into the almost transform-limited line C. In addition, this transition is known to arise from a single (axial) dipole moment [24, 25]. These properties are ideal for coupling to narrowband cavities and waveguides, and for single photon interface experiments including quantum cryptography. The following discussion therefore focusses on line C.

Over a period of 7 hours the line position was recorded for a single  $\text{SiV}^-$  center (Figure 3a). The variation in line position was found to be  $\pm 4$  MHz, which is within the 95% confidence interval for this parameter in a Lorentzian fit. The fact that we observe no spectral diffusion highlights the ability of  $\text{SiV}^-$  to produce indistinguishable photons over long periods of time. No blinking was observed for any of the  $\text{SiV}^-$  sites measured in this study.

PLE spectra were recorded for all 20 clearly-resolvable  $\text{SiV}^-$  sites in an arbitrary scan region, shown in Figure 3b. On a  $\{001\}$  surface the projections of  $\langle 111 \rangle$ -

aligned  $\text{SiV}^-$  centres form two orthogonal sets [24]. Scanning with two orthogonal laser polarisations (encoded in color) revealed the set to which each site in the region belonged [24]. The line position for each site is illustrated in Figure 3c. Within each orientation set the sites are closely spaced, although the distinct orientations are separated by about 5 GHz. Figure 3d shows a histogram of these shifts between consecutive sites. Out of the 20 centers, 11 pairs of  $\text{SiV}^-$  have separations less than one transform-limited FWHM. This means that for a randomly chosen site there is more than 50% probability of finding a second site in this scan region whose line is displaced by less than one FWHM. The two closest sites had lines separated by only 6 MHz (within the confidence interval of the fit), meaning a spectral overlap of at least 91%. Notably, this spectral overlap was achieved without external tuning of the spectral position.

To explain the observed homogeneity, we reconsider the energy level scheme in Figure 2b. The ground and excited states have E symmetry [15, 24, 25], and are split due to spin-orbit interaction [24]. In general, strain and electric fields can perturb these states to result in line-shifts and increased splittings. Electric fields may be produced by nearby charged impurities and therefore vary across small spatial scales. The precise correspondence between orientation and line position for each  $\text{SiV}^-$  measured here suggests that strain, which can be nearly uniform over a  $7 \times 7 \mu\text{m}$  region, is more influential than electric fields.

The large spin-orbit splittings of 46.68 GHz (258.1 GHz) in the ground (excited) state help to make  $\text{SiV}^-$  unresponsive to small transverse strains. This occurs because the effect of such strain is a small perturbation until strain splitting increases to about the magnitude of spin-orbit. We observed this effect in the ground-state splitting measured between lines C and D, which varied much less ( $\pm 1$  GHz) than line position

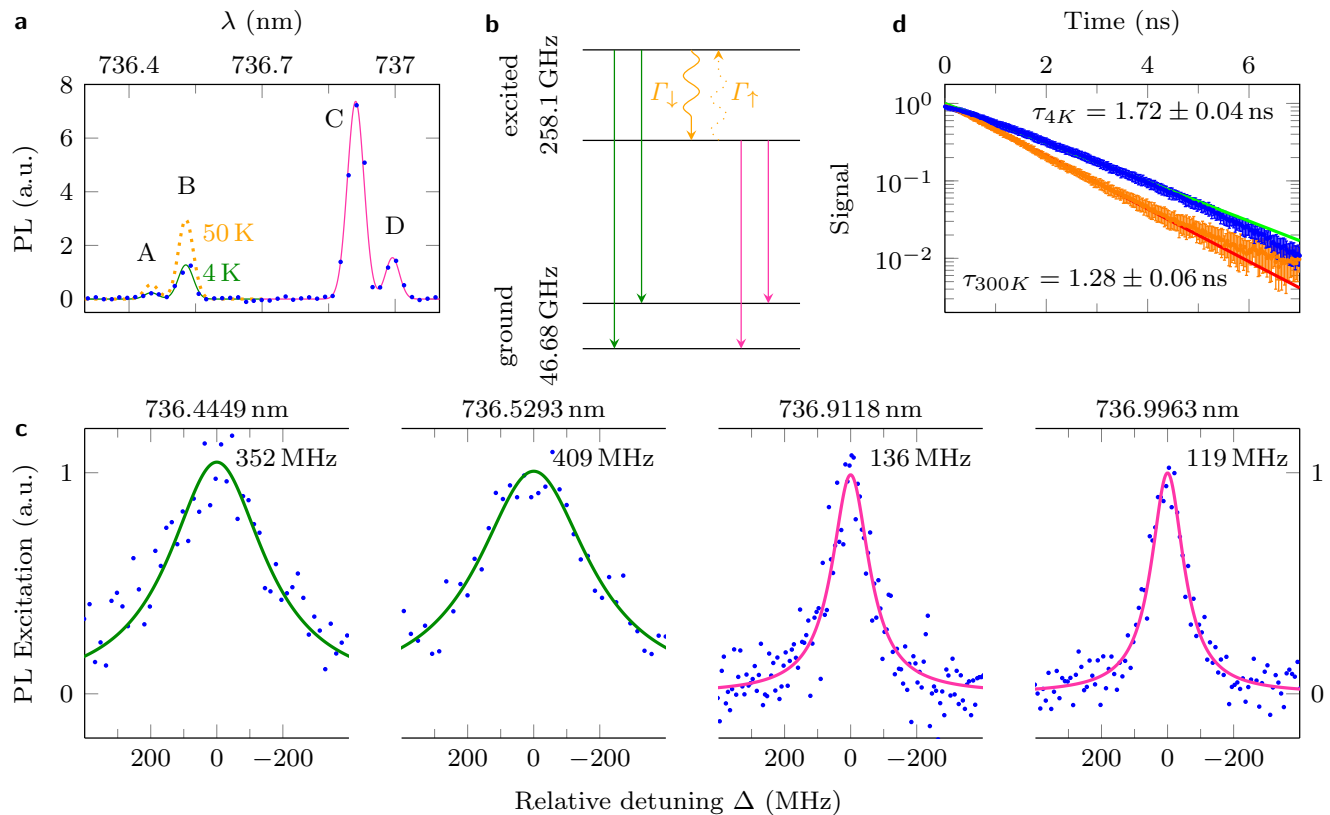


FIG. 2. Linewidths near the transform-limit. **a.** The  $\text{SiV}^-$  ZPL has a four-line fine structure (linewidth limited here by spectrometer resolution). The left-hand pair of lines are a mirror image of the right-hand pair, but they have much lower intensity at 4 K. These higher energy lines regain intensity with increasing temperature, and the dotted line illustrates the relative intensity at 50 K. **b.** This fine structure arises from transitions between a doublet excited state and a doublet ground state that both have zero-field splittings. Population is exchanged between the two excited state branches, but at low temperature the upward rate  $\Gamma_{\uparrow}$  is slow relative to the state lifetime. The downward exchange rate  $\Gamma_{\downarrow}$  dominates the relaxation within the excited state, which accounts for the loss of emission intensity for the high energy pair of lines. **c.** Excitation spectra of the four lines that comprise the  $\text{SiV}^-$  ZPL (amplitudes normalised). The higher energy lines are wider, consistent with a shorter effective lifetime due to thermalisation between the two excited state branches. **d.** The radiative decay lifetime of  $\text{SiV}^-$  increases from 1.28 ns at room temperature to 1.72 ns at 4 K, corresponding to a transform-limited PLE linewidth of 94 MHz.

across the 20 sites and showed no correlation with orientation. This implies that the observed line shift results from axial strain. The inversion symmetry of  $\text{SiV}^-$  [15, 24] reduces the influence of small axial strain, since inverting the strain direction does not change line shift. Our observations indicate that this shielding has a lower threshold than provided by spin-orbit for transverse strain. Despite the presence of residual strain in this sample region we were still able to find identical emitters.

An advantage to solid-state emitters over trapped ions is their reliable addressing which allows direct incorporation into photonic and plasmonic devices.  $\text{SiV}^-$  ensembles have been coupled into cavities [27], and here we incorporate single  $\text{SiV}^-$  centers into solid-immersion lens (SIL) to demonstrate their readiness for applications (Figure 4a). SILs allow increased collection of fluorescence from high refractive index materials [28], which is particularly useful during cryogenic experi-

ments. Well coupled  $\text{SiV}^-$  centers were identified by scanning the depth profile with a confocal microscope. The SIL enhanced fluorescence collection by about a factor of ten, giving saturation fluorescence up to  $I_{\text{sat}} = 730$  kilocounts/sec (kc/s). Using an oil-immersion objective on a flat surface,  $\text{SiV}^-$  produced  $I_{\text{sat}} = 200$  kc/s which is comparable to a single  $\text{NV}^-$  centre or bright molecule under the same conditions (Figure 4b).

The presence of poorly understood metastable states [29] prevents a deduction of absolute quantum yield for  $\text{SiV}^-$  from saturation fluorescence, although it appears to be less than the quantum yield for  $\text{NV}^-$  which has a fluorescence lifetime of 13 ns [12]. We found the  $\text{SiV}^-$  decay lifetime to be shorter ( $1.28 \pm 0.06$  ns) at room temperature than at 4 K (Figure 2d), This is consistent with a thermally activated non-radiative decay path [17, 26, 30], and indicates an improvement of the  $\text{SiV}^-$  quantum yield at low temperature. Our results show that  $\text{SiV}^-$  can provide indistinguishable photons at a collectable rate on the

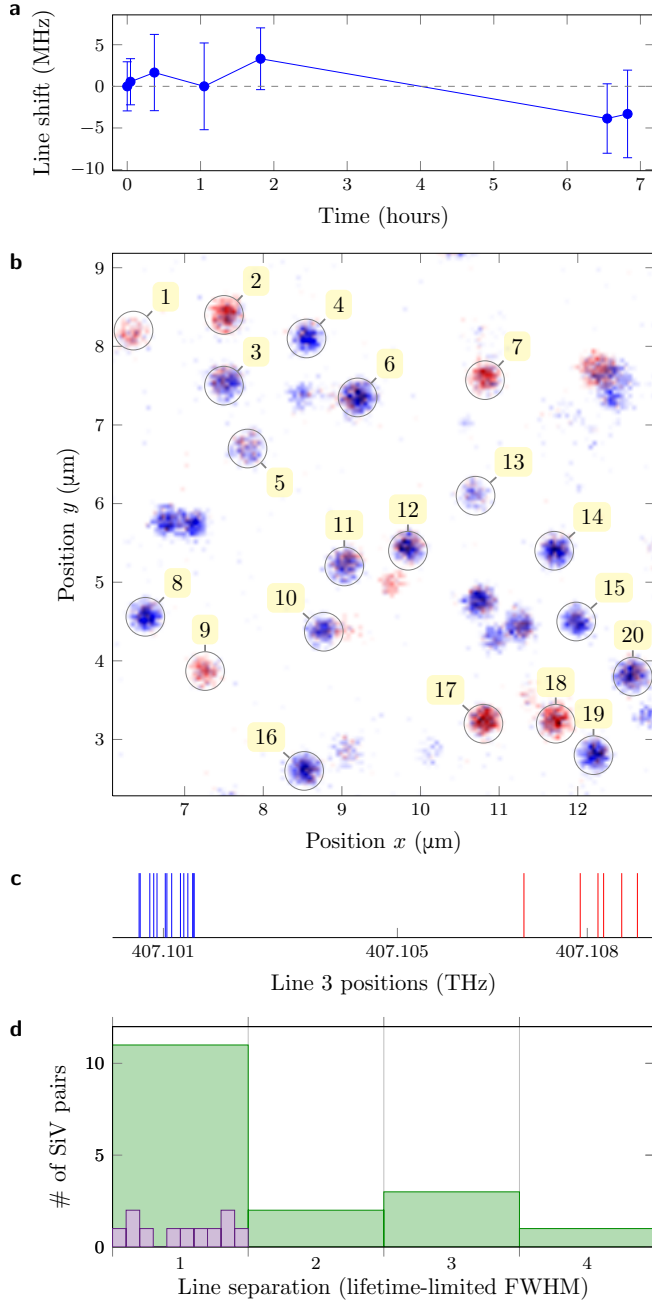


FIG. 3. Stability and uniformity of single SiV<sup>-</sup> centres. **a.** No measurable spectral diffusion was detected over a period of 7 hours. **b.** PLE spectra were measured for each of the 20 resolvable single SiV<sup>-</sup> centres in this confocal image (numbered). The image is a composite of two scans performed at orthogonal excitation polarisations, and so the apparent colour of the sites indicates its orientation in the crystal lattice. **c.** Position of line C for each of the 20 SiV<sup>-</sup> centers. **d.** Histogram of the shift between adjacent sites in **c.** The primary bins are 94 MHz wide corresponding to the transform-limited linewidth, and the composition of the first bin is illustrated in 10 sub-bins. Eleven SiV<sup>-</sup> pairs had separations less than 94 MHz, and four pairs had separations less than 30% of the lifetime-limited linewidth.

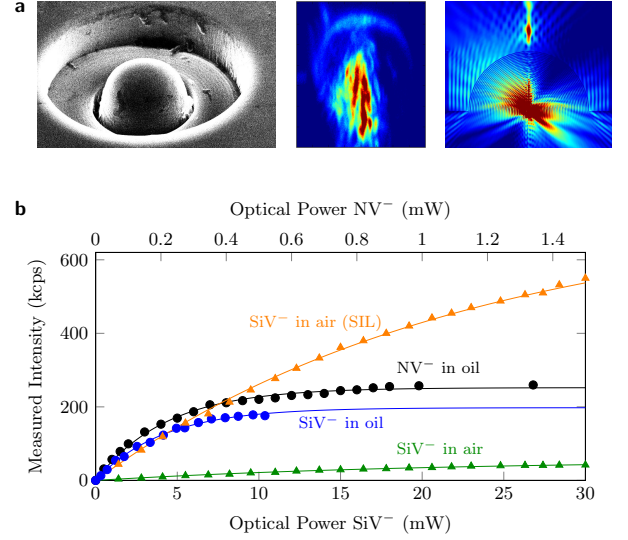


FIG. 4. SiV<sup>-</sup> incorporation into a SIL. **a.** Scanning electron microscope image of a single SIL fabricated in the diamond surface. The vertical cross-section confocal image (center) shows an intensity profile in the SIL with enhanced fluorescence detection for SiV<sup>-</sup> centres near the focus. This is in qualitative agreement with the simulated emission intensity (right) for a single dipole located at the centre of the solid immersion lens (calculated with finite-difference time-domain numerical package). **b.** Using an air objective (NA=0.95), the saturation count-rate  $I_{\text{sat}}$  for SiV<sup>-</sup> under a SIL (730 kc/s) is enhanced by more than a factor of 10 compared to an equivalent single SiV<sup>-</sup> under a planar surface nearby ( $I_{\text{sat}} = 56$  kc/s). To more easily compare SiV<sup>-</sup> with other emitters a high performance (NA=1.35) oil-immersion objective was used at room temperature. SiV<sup>-</sup> sites show  $I_{\text{sat}} = 200$  kc/s which is comparable to single NV<sup>-</sup> centers ( $I_{\text{sat}} = 252$  kc/s).

order of hundreds of kc/s.

In summary, we have demonstrated a uniform single photon source in the solid state without requiring external tuning of the optical properties. We observe nearly transform-limited linewidths, without spectral diffusion, which would allow high spectral overlap between single photons emitted from distinct sources. The production of multiple, independent single photon emitters with identical properties is essential to the scalability of a number of schemes that utilise entangled photons, including quantum computing with linear optics, and is expected to form a fundamental resource in quantum optics technologies. The SiV<sup>-</sup> center is therefore promising for such applications.

## METHODS

### Sample preparation

(001)-oriented plates cut from a low-strain, type-IIa, HPHT crystal (Sumitomo Electric Industries, Ltd.) were used as a substrate for microwave plasma chemical-vapour-deposition

(MPCVD). High-purity  $\text{H}_2$  and  $\text{CH}_4$  source gas, specified to 99.999%  $^{12}\text{C}$  isotopic enrichment (Cambridge Isotope Laboratories CLM-392) was used to produce the plasma. The residual  $\text{N}_2$  concentration was less than 0.1 ppb for  $\text{H}_2$  and less than 1 ppb for  $\text{CH}_4$ . The total gas pressure, microwave power, methane concentration ratio ( $\text{CH}_4/\text{H}_2$ ), growth duration and substrate temperature employed were 120 Torr, 1.4 kW, 4%, 24 h, and 950 – 1000 °C, respectively. The homoepitaxial layer thickness estimated from the weight difference between initial substrate and after the growth was  $\sim 60\text{ }\mu\text{m}$  giving a growth rate of  $2.4\text{ }\mu\text{m/h}$ .

Cathodoluminescence spectra (15 kV acceleration voltage,  $2 \times 10^{-7}\text{ A}$  incident beam current) taken at room temperature in a wavelength range from 200 – 800 nm provided information on the crystalline quality and optically active impurities. Emission from free-exciton recombination was observed from most of the growth surface, in addition to a weak signal at 738 nm which is assigned to  $\text{SiV}^-$ . The reaction vessel of MPCVD contains mainly stainless steel and molybdenum. Quartz glass ( $\text{SiO}_2$ ) was used for the windows of the vessel. When homoepitaxial film was grown under low microwave power, no  $\text{SiV}^-$  fluorescence was observed. Increasing the microwave input power caused the plasma to extend and etch material from the quartz, picking up silicon. In this study, a 6H-SiC single-crystal plate was also used as a Si source to allow increased silicon doping of grown diamond. The SiC plate was inserted between the diamond substrate and a molybdenum sample holder. It was possible to incorporate  $\text{SiV}^-$  during growth at concentrations below  $0.2/\mu\text{m}^3$  ( $\sim 1 \times 10^{-3}\text{ ppb}$ ). Incorporation of silicon occurred relatively uniformly over the whole lateral direction.

### Optical measurements

The sample was mounted in a continuous flow helium cryostat capable of cooling to 4 K. Single  $\text{SiV}^-$  centers were imaged using a home-built confocal microscope. The excitation laser beam (532 nm) was focussed onto the diamond surface through a 0.95

NA microscope objective (or 1.35 NA oil-immersion objective for room temperature measurements). The objective was scanned to produce confocal images of sample regions. Fluorescence was collected by the same objective, filtered with a 725–775 nm band-pass filter, and focused through a  $25\text{ }\mu\text{m}$  pinhole before detection on an avalanche photodiode (APD). After the pinhole the fluorescence could also be sent to a spectrometer to acquire spectra from single sites. Using a high resolution grating (1596 grooves/mm) allowed the four component fine-structure to be resolved.

Photoluminescent excitation (PLE) measurements were performed on the same setup, but using a Titanium:Sapphire laser with 50 kHz linewidth for excitation. This laser could scan across the entire ZPL, and detection was performed on the sideband by switching the filter to a 750–810 nm band-pass.

Decay lifetime of the excited state was measured by changing the excitation laser to a Ti:Sapph pumped optical-parametric-oscillator (OPO), producing 50 fs pulses at 80 MHz repetition rate. This OPO was set to 532 nm in order to excite  $\text{SiV}^-$  off-resonantly. The APD signal was analysed using a PicoQuant TimeHarp counting card, with a resolution of a 25 ps.

### SIL fabrication

SILs were produced in a region of the sample known to contain a medium density of  $\text{SiV}^-$  centres at a depth of 2.5–6  $\mu\text{m}$  below the surface. The site density was high enough to assure a reasonable probability of coupling a SIL to a colour centre. The fabrication process was performed with a Helios Nanolab 600 Focus Ion Beam (FIB) lithography system. Each SIL had a radius of  $7\text{ }\mu\text{m}$  and a depth of  $7\text{ }\mu\text{m}$ . The SIL images were taken with a Helios Nanolab 600 Focussed Ion Beam lithography system.

### REFERENCES

- [1] E. Knill, R. Laflamme, and G. J. Milburn, *Nature* **409**, 46 (2001).
- [2] Z.-S. Yuan, Y.-A. Chen, B. Zhao, S. Chen, J. Schmiedmayer, and J.-W. Pan, *Nature* **454**, 1098 (2008).
- [3] H. Bernien, B. Hensen, W. Pfaff, G. Koolstra, M. S. Blok, L. Robledo, T. H. Taminiau, M. Markham, D. J. Twitchen, L. Childress, and R. Hanson, *Nature* **497**, 86 (2013).
- [4] R. B. Patel, A. J. Bennett, I. Farrer, C. A. Nicoll, D. A. Ritchie, and A. J. Shields, *Nature Photonics* **4**, 632 (2010).
- [5] H. Bernien, L. Childress, L. Robledo, M. Markham, D. Twitchen, and R. Hanson, *Physical Review Letters* **108**, 043604 (2012).
- [6] A. Sipahigil, M. L. Goldman, E. Togan, Y. Chu, M. Markham, D. J. Twitchen, A. S. Zibrov, A. Kubanek, and M. D. Lukin, *Physical Review Letters* **108**, 143601 (2012).
- [7] C. Santori, D. Fattal, J. Vučković, G. S. Solomon, and Y. Yamamoto, *Nature* **419**, 594 (2002).
- [8] D. V. Strekalov, A. V. Sergienko, D. N. Klyshko, and Y. H. Shih, *Physical Review Letters* **74**, 3600 (1995).
- [9] J. Beugnon, M. P. A. Jones, J. Dingjan, B. Darquié, G. Messin, A. Browaeys, and P. Grangier, *Nature* **440**, 779 (2006).
- [10] A. J. Shields, *Nature Photonics* **1**, 215 (2007).
- [11] A. Kiraz, M. Ehrl, T. Hellerer, Ö. E. Müstecaplıoğlu, C. Bräuchle, and A. Zumbusch, *Physical Review Letters* **94**, 223602 (2005).
- [12] A. Faraon, C. Santori, Z. Huang, V. M. Acosta, and R. G. Beausoleil, *Physical Review Letters* **109**, 033604 (2012).
- [13] P. E. Barclay, K.-M. C. Fu, C. Santori, A. Faraon, and R. G. Beausoleil, *Physical Review X* **1**, 011007 (2011).
- [14] A. T. Collins, M. Kamo, and Y. Sato, *Journal of Materials Research* **5**, 2507 (1990).
- [15] J. P. Goss, R. Jones, S. J. Breuer, P. R. Briddon, and S. Öberg, *Physical Review Letters* **77**, 3041 (1996).
- [16] E. Neu, C. Hepp, M. Hauschild, S. Gsell, M. Fischer, H. Sternschulte, D. Steinmüller-Nethl, M. Schreck, and C. Becher, *New Journal of Physics* **15**, 043005 (2013).
- [17] T. Feng and B. D. Schwartz, *Journal of Applied Physics* **73**, 1415 (1993).
- [18] S. W. Brown and S. C. Rand, *Journal of Applied Physics* **78**, 4069 (1995).
- [19] C. D. Clark, H. Kanda, I. Kiflawi, and G. Sittas, *Physical Review B* **51**, 16681 (1995).
- [20] A. M. Edmonds, M. E. Newton, P. M. Martineau, D. J. Twitchen, and S. D. Williams, *Physical Review B* **77**, 245205 (2008).
- [21] E. Neu, D. Steinmetz, J. Riedrich-Möller, S. Gsell, M. Fischer, M. Schreck, and C. Becher, *New Journal*

- of Physics **13**, 025012 (2011).
- [22] A. V. Turukhin, C.-H. Liu, A. A. Gorokhovsky, R. R. Alfano, and W. Phillips, Physical Review B **54**, 16448 (1996).
  - [23] C. Wang, C. Kurtsiefer, H. Weinfurter, and B. Burchard, Journal of Physics B: Atomic, Molecular and Optical Physics **39**, 37 (2006).
  - [24] L. J. Rogers, K. D. Jahnke, M. W. Doherty, A. Dietrich, L. P. McGuinness, C. Müller, T. Teraji, H. Sumiya, J. Isoya, N. B. Manson, and F. Jelezko, Physical Review B **89**, 235101 (2014).
  - [25] C. Hepp, T. Müller, V. Waselowski, J. N. Becker, B. Pingault, H. Sternschulte, D. Steinmüller-Nethl, A. Gali, J. R. Maze, M. Atatüre, and C. Becher, Physical Review Letters **112**, 036405 (2014).
  - [26] A. T. Collins, L. Allers, C. J. Wort, and G. A. Scarsbrook, Diamond and Related Materials **3**, 932 (1994).
  - [27] J. C. Lee, I. Aharonovich, A. P. Magyar, F. Rol, and E. L. Hu, Optics Express **20**, 8891 (2012).
  - [28] L. Marseglia, J. P. Hadden, A. C. Stanley-Clarke, J. P. Harrison, B. Patton, Y.-L. D. Ho, B. Naydenov, F. Jelezko, J. Meijer, P. R. Dolan, J. M. Smith, J. G. Rarity, and J. L. O'Brien, Applied Physics Letters **98**, 133107 (2011).
  - [29] E. Neu, R. Albrecht, M. Fischer, S. Gsell, M. Schreck, and C. Becher, Physical Review B **85**, 245207 (2012).
  - [30] L. Rogers, Physics Procedia **3**, 1557 (2010).

## ACKNOWLEDGEMENTS

We acknowledge ERC, EU projects (SIQS, DIADEMS, EQUAM), DFG (FOR 1482, FOR 1493 and SFBTR 21), JST,BMBF, the Alexander von Humboldt, and the Sino-German and Volkswagen foundations for funding. We acknowledge G. Neusser and the FIB Center UUlM for support manufacturing SILs.